Proceedings of ASME Turbo Expo 2011
GT2011
June 6-10, 2011, Vancouver, British Columbia, Canada

GT2011-45664

BUNSEN FLAME BLOW-OFF: VELOCITY-MATCHING METHOD

Huang Xia*, Huang Yong, Wang Fang, Hu Bin

National Key Laboratory on Aero-engines, School of Jet Propulsion,
Beihang University, 100191 Beijing, China

ABSTRACT

The effect of the incoming velocity on the anchoring point of a Bunsen flame is studied by theoretical analysis and experiments, since the anchoring point is essential to the flame holding. In order to predict the locations of the anchoring point, the velocity-matching (VM) method, which compares the profile of the flow velocity of the cold flow with that of the flame speed near the exit of a Bunsen burner, is employed together with the consideration of the cold wall quenching. The anchoring point is predicted to be located at

$$\begin{cases} x = C_{x1}u_0 + C_q d_{q0} u_0^{1/2} + C_{x2} d_{q0} \\ y = -C_{y1} S_{L0}^{1/2} u_0^{-1} + C_{y2} S_{L0} u_0^{-2} + C_{y3} S_{L0}^{1/2} u_0^{-2} + C_{y4} \end{cases} .$$

The experiment on the variation of the anchoring point with the incoming gas velocity is done with a laminar premixed methane-air flame. The equivalence ratios of the pre-mixture are 1.0, 0.9, and 0.8, respectively, and the incoming velocity is less than 2.00 m/s *in the experiment. The results show that the anchoring point moves downstream and towards instead of away from the centerline of the jet as estimated by Bernard Lewis with increasing incoming gas velocity. The prediction of the locations of the anchoring point by VM method agrees well with the experiment within the uncertainty of less than ±20%.*

Keywords: *velocity-matching; flame anchoring point; Bunsen burner; laminar premixed flame*

NOMENCLATURE

a	thermal diffusivity
D	mass diffusivity
d	burner exit diameter
d_q	quenching distance
h	heat convection coefficient
Pr	Prandtl number
Re	Reynolds number
RR	chemical reaction rate
Sc	Schmidt number
S_L	flame speed
u	flow velocity
Y	fuel concentration
α	outer border angle of free jet
δ	thickness of boundary layer
θ	inner border angle of free jet
λ	heat conduction coefficient
ϕ	equivalence ratio
ν	kinematic viscosity
(x, y)	coordinates of the anchoring point

Subscripts

0	initial value
q	quenching
Y	concentration

INTRODUCTION

In order to reduce NOx emissions, in modern aero-engine combustor designs the fuel is burnt close to lean blow-off limit to control the temperature. One of the technology is the LPP

* Address all correspondence to this author.

(Lean Premixed and Pre-vaporized) combustors. However, the flame is unstable when the equivalence ratio is close to lean blow-off limit. Such technology calls for high precision prediction of lean blow-off limit. On the other hand, lean blow-off is important not only in low emission combustors, but also in conventional gas turbine combustors. The operation condition of an aero engine is often changed widely during a flight cycle. In order to have the flame stabilized in the entire cycle, lean blow-off limit should be known accurately.

An underlying concept of the gas turbine combustor lean blow-off limit is that the flame blows off when the heat released in the combustor could not heat the fresh premixed gas to the reaction temperature. For heterogeneous mixtures Lefebvre [1] suggested as the following expression for lean blow-off limit,

$$q_{LBO} = \left[\frac{A'' f_{pz}}{V_{pz}}\right]\left[\frac{\dot{m}_A}{P_3^{1.3}\exp(T_3/300)}\right]\left[\frac{D_0^2}{\lambda_{eff} LCV}\right] \quad (1)$$

where A'' is fixed by experiment.

The models of combustor lean blow-off are mainly developed from the analysis of bluff body flame-holders. One is Longwell's [2] well-stirred reactor model, which gives a correlation as

$$\frac{u_{BO}}{P^{n-1}D_c} = f(\phi_{BO}) \quad (2)$$

The other is recirculation-ignition model first proposed by Zukowski and Marble [3]. Similar to the well-stirred reactor model, the equation is

$$\frac{u_{BO}}{PD_c} = f(T) \quad (3)$$

where u_{BO} is the blow-off velocity, P is the pressure, D_c is the characteristic scale of the flame-holder, ϕ_{BO} is the blow-off equivalence ratio, and T is the temperature. ϕ_{BO} is a function of T. Both of these two models are based on the conservation of the heat energy, thus their results are similar. Up to the present, the lean blow-off models have been proposed based on the ideas above.

However, these models have some limitations either for bluff body flame-holders or combustors, as they ignore some essential factors of flame-holding. The flame propagates as a wave and is anchored where the flow velocity is balanced with the flame speed. However, this velocity-balance mechanism is absent in Eqs. (1), (2), and (3).

In fact, Lewis and von Elbe [4, 5] have studied the flame-holding mechanism of Bunsen flame. For a typical Bunsen flame, the flame anchoring point is at the root of the flame. The existence of this point determines the existence of the flame.

Lewis et al. suggested a plot as Fig. 1. The flow velocity and the flame speed have been plotted as functions of distance from the stream boundary. For any gas velocity curve above curve 2 there is an anchoring point of the flame above the orifice, as indicated by positions A, B, and C. As the flow velocity increases, the flame speed curve progressively moves toward the boundary until a critical flow velocity corresponding to curve 4 is reached. If the flow velocity is further increased (curve 5), the flow velocity exceeds the flame speed everywhere, then the flame blows off. [5]

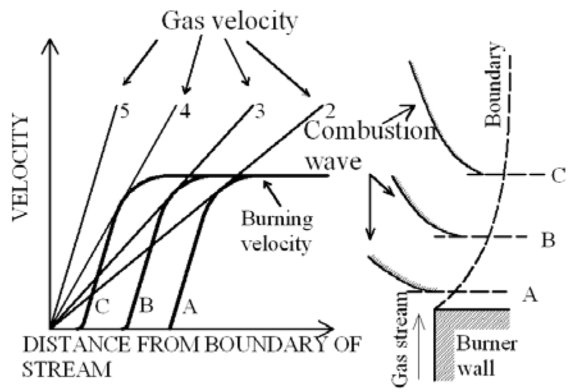

Figure 1. FLOW VELOCITY AND FLAME SPEED PROFILES OUTSIDE BURNER [5].

Wohl [6] developed Lewis's model. His analysis is based on Fig. 2, in which point A is the anchoring point in Lewis's theory. In area ACDB the flame speed is greater than the local flow velocity. Once ignited in this area, the flame will flash back and stop at point A. If ignited out of this area, the flame will blow off. Thus, area ACDB is called the ignition area. The ignition area decreases with increasing gas velocity. When the ignition area decreases to a point, the flame blows off. Both Wohl's and Lewis's models have shown that the flame holding mechanism is determined by the existence of the anchoring point.

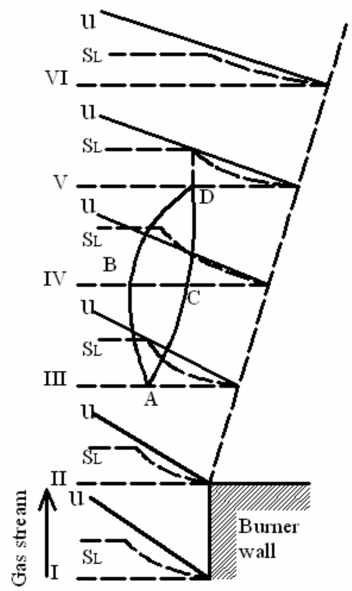

Figure 2. WOHL'S EXPLANATION ON FLAME BLOW-OFF [6].

Although Lewis's and Wohl's models explain the flame-holding mechanism qualitatively, they are not capable to provide quantitative prediction of the blow-off limit. There are few correlations related to basic combustion concepts such as the flame speed, the quenching distance, and the flammability limit. The descriptions of flame lean blow-off mechanism in most recent literature are similar to that of Lewis's model, as in [6-9].

This paper studies the anchoring point of a laminar lean premixed Bunsen flame by both theoretical and experimental methods. The flame anchoring point is the root of the ignition area, and the critical condition of the ignition area is the blow-off limit. Therefore, the results of the anchoring point are helpful for further understanding the mechanism of flame-holding, including the accurate prediction of laminar lean blow-off limit. Besides, the mechanism of turbulent flame-holding is also the balance of velocity. The main difference between turbulent and laminar conditions may be that the flow field of the turbulent flame is much more complicated than that of the laminar flame. Thus once the instantaneous turbulent flow field is achieved, the method of predicting laminar lean blow-off limit should be applied to the turbulent cases, such as in gas turbine combustors.

1. VELOCITY-MATCHING METHOD

In this paper, a velocity-matching method (VM method) is used to predict the anchoring point of a typical conical Bunsen flame which is lifted about 1mm away from the burner. First, the incoming flow velocity and the flame speed profiles are plotted downstream of the burner. These two velocity profiles may have intersection points. At these points the flow velocity is in equilibrium with the flame speed. This is the necessary condition of flame-holding. Then, if at an intersection point the flame can be held when subjected to any disturbances, this point is the flame anchoring point.

1.1. COORDINATE SYSTEM

In order to plot the flow velocity and the flame speed profiles, the coordinate system near the exit of the Bunsen burner is established. Only half of the field was studied due to symmetry. The origin is at the rim of the inner wall. X-axis points to the flow direction and y-axis is towards the centerline of the burner.

1.2. JET BOUNDARY LAYER

The anchoring point is expected to be in the boundary layer immediately downstream the burner exit. Therefore, the detailed flow field of the boundary layer is analyzed as follows.

1.2.1. FLOW VELOCITY

It is well known that there is a core flow in which the flow velocity is the same as the exit velocity u_0. Outside the core flow zone, there is a boundary layer where the velocity decreases because of the momentum transport between the gas jet and the surrounding air. The border between the boundary and the surrounding air is called the outer border, on which the flow velocity is 0. The border between the boundary and the core flow is called the inner border, on which the flow velocity is u_0. In the field immediately downstream the burner, the boundary scale is much smaller than the burner diameter. Besides, the Reynolds number is not more than 2300 (the flow velocity is less than 2m/s and the diameter of the burner exit is 10mm), which means the flow is laminar in this study [10]. And the flame will be lifted some distance above the tube so that the thermal expansion can be ignored [11]. Thus, according to the theory of laminar free jet the outer and the inner borders can be simplified to be two straight lines with constant spread angles. And the velocity profiles can also be assumed to be straight lines, as discussed in [5, 6]. Thus, as shown in Fig. 3, the angle α between the outer border and x-axis is determined by

$$\tan\alpha = C_\alpha \nu \tag{4}$$

where ν is the kinematic viscosity of the premixed gas.

Similarly, the angle θ between the inner border and x-axis is determined by

$$\tan\theta = C_\theta \nu \tag{5}$$

The thickness of the velocity boundary layer at the exit plane of the burner is

$$\delta_0 = C_\delta \nu \tag{6}$$

The lines of the outer and the inner borders can be written as

$$y = -\tan\alpha x = -C_\alpha \nu x \tag{7}$$

and

$$y = \tan\theta x + \delta_0 = C_\theta \nu x + C_\delta \nu \tag{8}$$

respectively.

Then the velocity at any point (x, y) in the boundary is given as

$$u = \frac{C_\alpha \nu x + y}{(C_\alpha + C_\theta)\nu x + C_\delta \nu} u_0 \tag{9}$$

In Eqs. (4) to (9), C_α, C_θ and C_δ are constants.

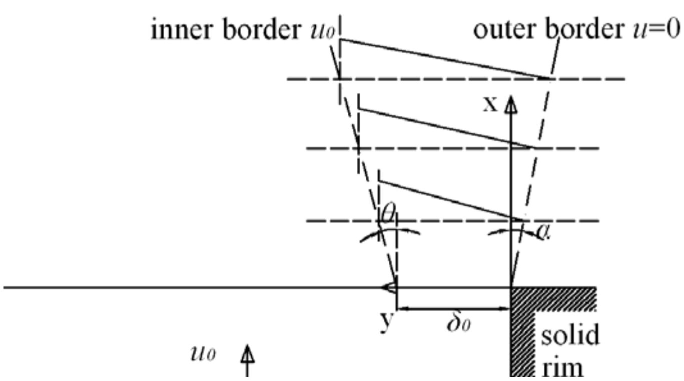

Figure 3. VELOCITY PROFILES IN THE BOUNDARY LAYER DOWNSTREAM THE BURNER EXIT.

1.2.2. FUEL CONCENTRATION

The flame speed $S_L \propto \sqrt{a \cdot RR}$. The reaction rate RR is related to the temperature and the concentration. There is

$$RR \propto f(T)\cdot Y. \tag{10}$$

In this case the initial temperature of the pre-mixture is supposed to be uniform, thus to lean flames the chemical reaction rate is only proportional to the fuel concentration Y. Consequently, the fuel concentration profiles are similar to the flame speed profiles.

The contour of the fuel concentration is normal to the solid wall as the fuel cannot penetrate the wall. Then the fuel concentration profiles can be plotted as Fig. 4. The red and black lines are the concentration and the velocity profiles, respectively. Similar to the descriptions in Section 1.2.1, the angle α_Y between the concentration outer border and x-axis and the angle θ_Y between the inner border and x-axis are determined by

$$\tan\alpha_Y = C_\alpha D \tag{11}$$

and

$$\tan\theta_Y = C_\theta D \tag{12}$$

respectively.

The thickness of the concentration boundary layer at the exit plane of the burner is

$$\delta_{Y0} = 2C_\delta D \tag{13}$$

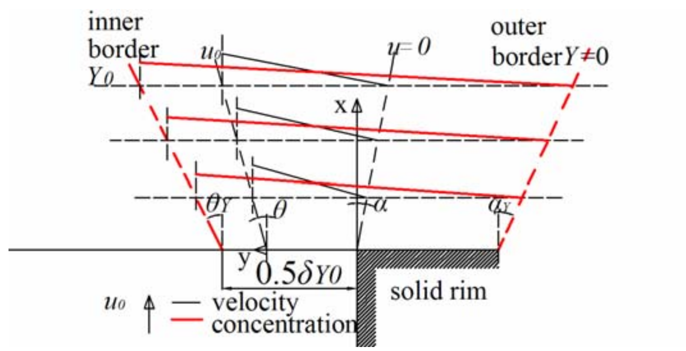

Figure 4. VELOCITY AND CONCENTRATION PROFILES IN BOUNDARIES DOWNSTREAM THE BURNER EXIT.

The lines of the outer and the inner borders are given by

$$y = -\tan\alpha_Y x - 0.5\delta_{Y0} = -C_\alpha D x - C_\delta D \tag{14}$$

and

$$y = \tan\theta_Y x + 0.5\delta_{Y0} = C_\theta D x + C_\delta D \tag{15}$$

respectively.

The fuel concentration at any point (x, y) in the boundary is

$$Y = \frac{C_\alpha D x + y + C_\delta D}{(C_\alpha + C_\theta) D x + 2C_\delta D} Y_0 \tag{16}$$

1.3. PRIMARY ANALYSIS

Comparing the profiles of the flow velocity and the flame speed will give all equilibrium points. The locus of all these points is shown as the blue dashed curve 1 in Fig. 5.

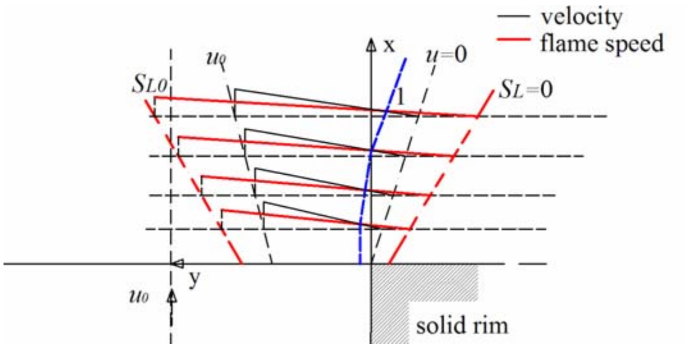

Figure 5. FLOW VELOCITY AND FLAME SPEED PROFILES DOWNSTREAM THE BURNER EXIT.

In Figure 5, on the left side of the curve 1 and the right side of that denoted by S_L=0, the flow velocity is greater than the flame speed. Any flame will blow off. Between these two curves the flow velocity is less than the flame speed, so that a flame will flash back. However, these two curves are not closed upstream, implying that the flame will always flash back into the burner. Obviously, this is not true. Therefore, there must be some additional factors to anchor the flame.

1.4. WALL QUENCHING AND THE ANCHORING POINT

In a critical distance near wall, the flame can not exist due to wall quenching [6]. The influence of wall quenching to the velocity matching is shown in Fig. 6, where d_q is the quenching distance. d_q is assumed to be the same along the solid rim. Therefore, the border of the quenching area is shown as curve 2 in Fig. 6. Curve 2 is simplified as straight lines parallel to the solid rim with circular arc at the corner. In this distance around the burner wall, the flame speed is 0. Curves 1 and 2 intersect at point P1. Similar to the analysis for Fig. 5, the flame blows off outside the area surrounded by curves 1, 2, and 3. If ignited inside this area, the flame will move upstream and be anchored at point P1. At this point the flame is stable under any disturbances. Therefore, point P1 is the flame anchoring point and the area surrounded by curves 1, 2, and 3 is the ignition area.

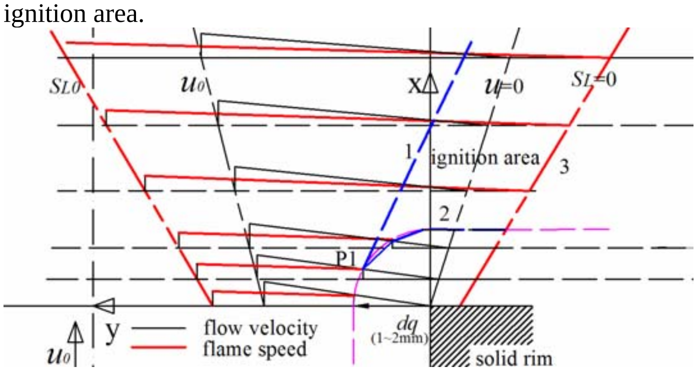

Figure 6. FLOW VELOCITY AND FLAME SPEED PROFILES CONSIDERING WALL QUENCHING.

1.5. DETAILED ANALYSIS

Based on the analysis above, the magnitude of the flow velocity is equal to the flame speed at the anchoring point, i.e.

$$u(x,y) = S_L(x,y) \tag{17}$$

The profile of the flame speed in the concentration boundary layer is given by [12]

$$S_L = \frac{(a \cdot RR)^{1/2}}{(a_0 \cdot RR_0)^{1/2}} S_{L0} \tag{18}$$

where S_{L0} is the flame speed for Y_0.

Then Eqs. (10), (17) and (18) give

$$u(x,y) = S_L(x,y) = (Y/Y_0)^{1/2} S_{L0} \tag{19}$$

and according to Eq. (16),

$$(Y/Y_0)^{1/2} = \left(\frac{C_\alpha Dx + y + C_\delta D}{(C_\alpha + C_\theta)Dx + 2C_\delta D} \right)^{1/2}$$

The wall quenching effect will suppress the flame formation around point P1 within a range

$$(x^2 + y^2)^{1/2} = d_q \tag{20}$$

where d_q is related with the flow velocity u_0. d_q increases with increasing u_0, since the heat transfer from the jet to the cold wall is strengthened. According to [13, 14], the quenching distance can be determined as

$$(x^2+y^2)^{1/2} = d_q = C_q d_{q0} u_0^{1/2} + \left((C_q d_{q0} u_0^{1/2})^2 + d_{q0}^2 \right)^{1/2} \tag{21}$$

where $C_q = 0.664(a/d)^{1/2} RR^{-1}$, d is the exit diameter of the burner, and d_{q0} is the quenching distance of the quiescent gas. C_q shows that the quenching distance will increase if the heat released by reaction decreases or the heat loss of the system increases. This assumption may be too simple. However, the wall quenching effect itself has not been studied perfectly enough [6, 15].

Combining Eqs. (19) and (21) results in

$$\begin{cases} u(x,y) = S_L(x,y) = (Y/Y_0)^{1/2} S_{L0}, \\ (x^2+y^2)^{1/2} = d_q = C_q d_{q0} u_0^{1/2} + \left((C_q d_{q0} u_0^{1/2})^2 + d_{q0}^2 \right)^{1/2} \end{cases} \tag{22}$$

Substituting $(Y/Y_0)^{1/2}$ and C_q in Eqs. (22) and simplifying them by Taylor expansion yields

$$\begin{cases} x = C_{x1} d_{q0} u_0 + C_q d_{q0} u_0^{1/2} + C_{x2} d_{q0}, \\ y = C_{y1} S_{L0}^{-1/2} u_0^{-1} \\ \quad - C_{y1} S_{L0}^{-1/2} u_0^{-2} - C_{y2} S_{L0} u_0^{-2} + C_{y3} S_{L0}^{1/2} u_0^{-2} + C_{y4} \end{cases} \tag{23}$$

Eqs. (23) are the correlations to predict the location of the anchoring points. In these equations,

$$C_q = 0.664 (a/d)^{1/2} RR^{-1} \tag{24}$$

$$C_{x1} = \frac{C_q^2}{2(C_q^2+1)^{1/2}} \tag{25}$$

$$C_{x2} = 0.5 (C_q^2 + 1)^{1/2} - 0.5 \tag{26}$$

$$C_{y1} = \frac{2.5 C_3 C_q d_{q0} + 2 C_1^2 C_2}{(8 C_2 C_3 C_q d_{q0} + 8 C_1^2 C_2^2 + C_1^4 S_{L0})^{1/2}} \tag{27}$$

$$C_{y2} = 0.25 C_1^2 / C_2 \tag{28}$$

$$C_{y3} = 0.25 \times (8 C_2^{-1} C_3 C_q d_{q0} + 8 C_1^2 + C_1^4 C_2^{-2} S_{L0})^{1/2} \tag{29}$$

$$C_1 = C_\delta \nu \tag{30}$$

$$C_2 = C_\delta D \tag{31}$$

$$C_3 = C_\delta^2 \nu^2 C_\alpha D + 2(C_\alpha + C_\theta) \nu C_\delta \nu C_\delta D \tag{32}$$

and C_{y4} is determined from the experiments in the next section.

C_α, C_θ, and C_δ are constants of laminar free jet. Here $C_\alpha \nu = 0.2282$, $C_\theta \nu = 0.0987$, and $C_\delta \nu = 0.0018$ m.

a and ν are calculated from methane and air mixtures. $a = 2.14 \times 10^{-7}$ m^2/s, $\nu = 1.506 \times 10^{-5}$ m^2/s.

Sc is assumed to be 0.7. S_{L0}, and d_{q0} are parameters of methane [16]. Y_0 is the fuel concentration. d is the inner diameter of the burner exit. Substituting these parameters into the constants above gives

$C_q = 0.681$ (s/m)$^{0.5}$,

$C_{x1} = 0.192$ s, $C_{x2} = 0.105$,

$d_{q0} = 0.0019$ m. $C_1 = 0.0018$ m, $C_2 = 0.0026$ m, $C_3 = 4.12 \times 10^{-6}$ m^2

$C_{y1} = 1.47 \times 10^{-4}$ m$^{3/2}$s$^{-1/2}$, $C_{y2} = 3.12 \times 10^{-4}$ m^2/s, $C_{y3} = 6.38 \times 10^{-5}$ m$^{5/2}$s$^{-3/2}$,

Therefore, Eqs. (23) can be written as

$$\begin{cases} x = 3.642 \times 10^{-4} u_0 + 1.294 \times 10^{-3} u_0^{1/2} + 0.105 d_{q0}, \\ y = 1.773 \times 10^{-3} S_{L0}^{-1/2} u_0^{-1} - 1.773 \times 10^{-3} S_{L0}^{-1/2} u_0^{-2} - 3.115 \times 10^{-4} S_{L0} u_0^{-2} \\ \quad + 1.636 \times 10^{-3} S_{L0}^{1/2} u_0^{-2} + C_{y4} \end{cases} \tag{33}$$

According to Eqs. (33), if the flow velocity increases, the anchoring point will move downstream and towards the centerline of the jet, which is contrary to Lewis's analysis.

2. EXPERIMENTAL VALIDATION

2.1. TEST CONDITIONS

A Series of Bunsen flame experiments have been conducted to validate the correlation of Eqs. (33). In the experiments methane is used as the fuel and the locations of the anchoring points under different flow velocities have been measured when the equivalence ratios of the methane-air mixture are 1.0, 0.9, and 0.8, respectively. The blow-off velocity are 1.75m/s, 1.16m/s, and 0.66m/s when ϕ=1, 0.9, and 0.8, respectively.

2.2. EXPERIMENTAL SETUP

The schematic diagram of the experiment is shown in Fig. 7. Methane and air are stocked in two high pressure cans 1 and 2. Can 3 is a pre-mixture container. Before the experiment methane and air are released to can 3 respectively. The equivalence ratio of the pre-mixture is controlled based on the partial pressures of methane and air. The flowmeters 9 and 10 are used to measure and control the flow velocity. The inner diameter of the burner exit is 10mm. The locations of the anchoring points are photographed by a NIKON COOLPIX P90 camera with 4, 000×3, 000 pixels. The exposure time is 1/6s in order to obtain steady photos of the flame. No filter is used.

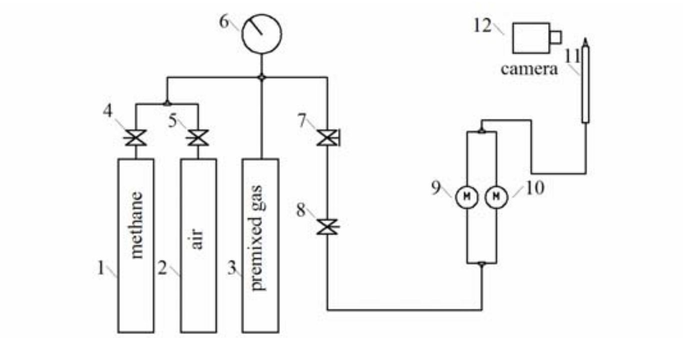

Figure 7. BUNSEN FLAME EXPERIMENT.
1, 2, 3-gas can; 4, 5, 7, 8-valve; 6-piezometer; 9, 10-flowmeter; 11-Bunsen burner; 12-camera.

The method the anchoring points being determined is shown in Fig. 8. A borderline can be achieved after running "color difference" order in the flame photo, as red line in Fig. 8. The anchoring point of the flame is determined to be the point the closest to the solid rim.

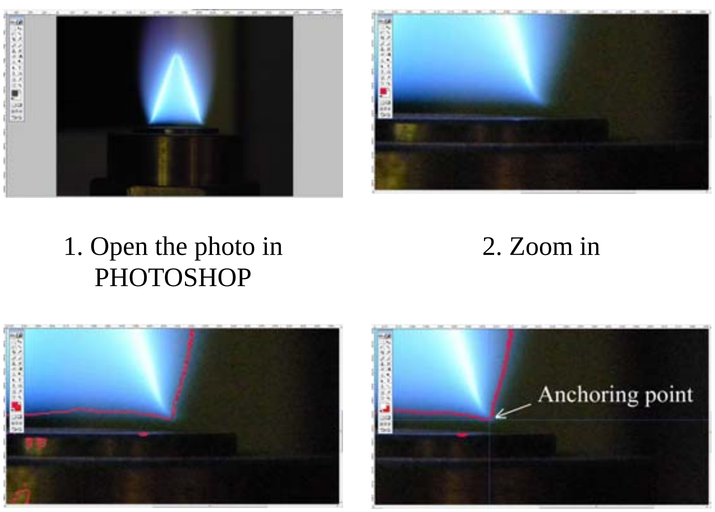

1. Open the photo in PHOTOSHOP

2. Zoom in

3. Run "color difference" order

4. Determine the anchoring point

Figure 8. THE METHOD OF DETERMINING THE ANCHORING POINT.

2.3. EXPERIMENTAL RESULTS

The locations of anchoring point can be plotted as shown in Fig. 9. This figure shows the anchoring point locations with u_0 for ϕ =1.0. Similarly, the anchoring point locations with u_0 for ϕ =0.9 and 0.8 are shown in Figs. 10 and 11, respectively.

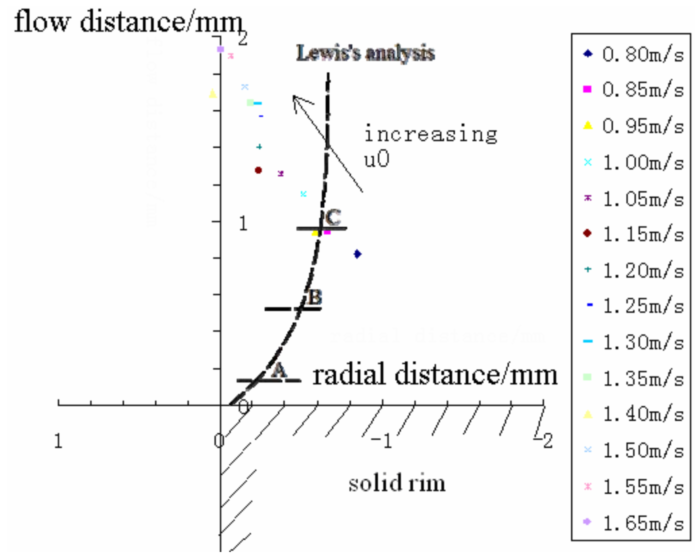

Figure 9. ANCHORING POINT LOCATIONS FOR ϕ =1.0.

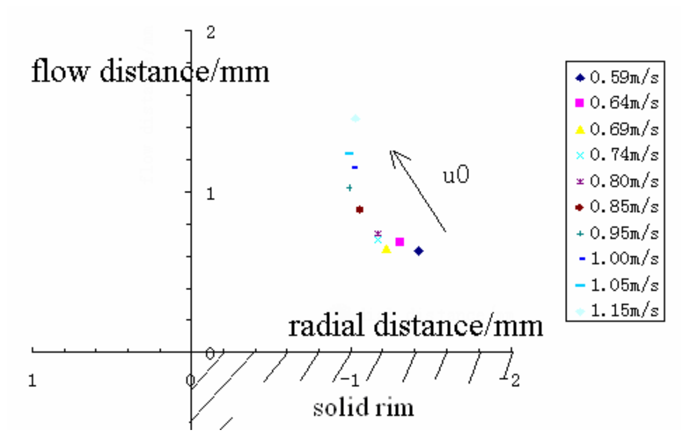

Figure 10. ANCHORING POINT LOCATIONS FOR ϕ =0.9.

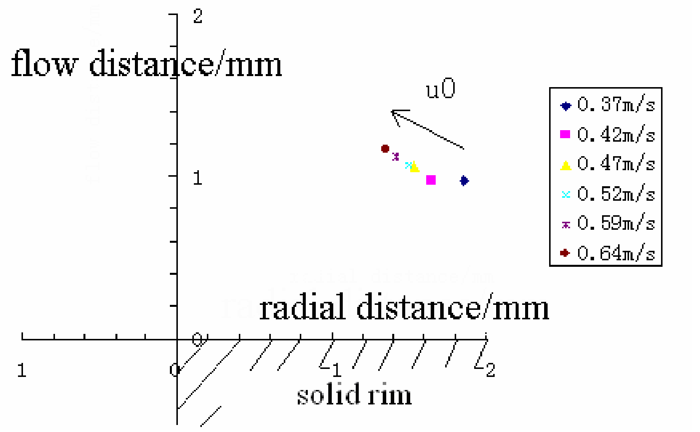

Figure 11. ANCHORING POINT LOCATIONS FOR ϕ=0.8.

The results indicate that when the flow velocity increases, the anchoring points will move downstream and towards instead of away from the centerline of the jet as estimated in Lewis's theory.

3. VELOCITY-MATCHING PREDICTION

The constant C_{y4} is determined as 0.0004m from the experiments in section 2.

Substituting C_{y4} into Eqs. (33) can result in

$$\begin{cases} x = 3.642\times10^{-4}u_0 + 1.294\times10^{-3}u_0^{1/2} + 0.105d_{q0}, \\ y = 1.773\times10^{-3}S_{L0}^{-1/2}u_0^{-1} - 1.773\times10^{-3}S_{L0}^{-1/2}u_0^{-2} - 3.115\times10^{-4}S_{L0}u_0^{-2} \\ \quad + 1.636\times10^{-3}S_{L0}^{1/2}u_0^{-2} - 0.0004 \end{cases} \tag{34}$$

where the flame speed S_{L0} depends on the equivalence ratio ϕ. The comparisons between the experiments and the predictions for ϕ=1.0, 0.9, and 0.8 are shown in Fig. 12.

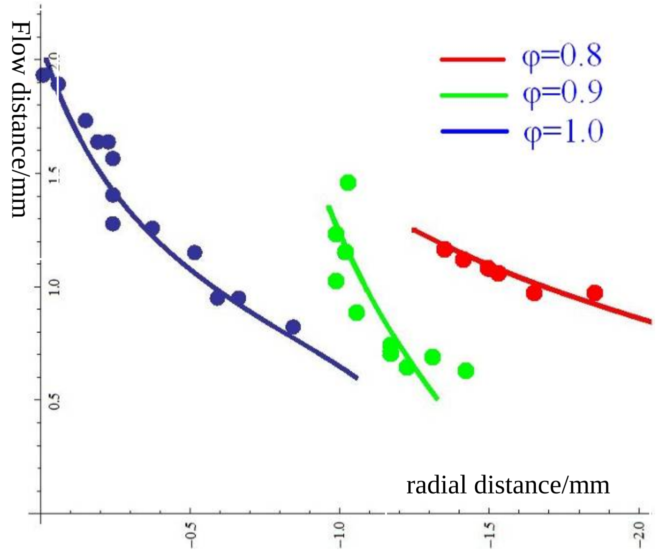

Figure 12. ANCHORING POINT LOCATIONS AND THEORETICAL CURVE FOR ϕ=1.0, 0.9, and 0.8.

It is seen that the theoretical predictions of the locations of the anchoring points by VM method agree well with the experiments. The uncertainties by predictions are ±11.2%, ±12.5%, and ±20% for ϕ=1.0, 0.9, and 0.8, respectively. However, the agreement is poorer for lower velocity. The possible reason is that the thermal expansion becomes more important when the flame is too close to the solid rim.

The result that the anchoring points move towards instead of away from the jet centerline with increasing incoming flow velocity is contrary to the analysis of Lewis and von Elbe. This is the result of the expansion of the wall quenching area. In Eq. (21), the quenching distance increases with the flow velocity. The increasing quenching area cuts part of the flame root, therefore the anchoring point moves towards the centerline.

4. CONCLUSIONS

In order to study the mechanism of flame-holding and predict lean blow-off limits, a VM method is used in a Bunsen flame. This method yields a prediction of the anchoring point locations. Then an experiment of Bunsen flames is conducted to validate the theoretical prediction. The conclusions are as follows.

(1) The predicted location of the anchoring point is

$$\begin{cases} x = C_{x1}d_{q0}u_0 + C_q d_{q0}u_0^{1/2} + C_{x2}d_{q0}, \\ y = C_{y1}S_{L0}^{-1/2}u_0^{-1} - C_{y1}S_{L0}^{-1/2}u_0^{-2} - C_{y2}S_{L0}u_0^{-2} + C_{y3}S_{L0}^{1/2}u_0^{-2} + C_{y4} \end{cases}$$

.

It is clearly shown that the basic combustion concepts such as the flame speed S_L and the quenching distance d_q are involved in the correlation.

(2) For the laminar premixed methane-air Bunsen flame, the anchoring point moves downstream and towards instead of away from the jet centerline with increasing incoming flow velocity. That is contrary to the analysis of Lewis and von Elbe.

(3) The uncertainties of velocity-matching method are ±11.2%, ±12.5% and ±20% while ϕ =1.0, 0.9, and 0.8, respectively.

In the introduction the flame blows off while the ignition area becomes one point. The anchoring point is only the lowest position of the ignition area. In order to predict the blow-off velocity the location of a highest position needs to be calculated by VM method. This position may be influenced by the flammability limit of the fuel. It is the next topic for the authors to predict the lean blow-off limit of Bunsen flame.

The conclusions above are for the laminar flames. Theoretically, VM method is also suitable for the turbulent flames. However, the instantaneous flow field of turbulent flow is more complicated than that of laminar flow. The flame may be locally extinguished but still anchored above the burner exit globally. Thus the theory about local extinguish must be considered in turbulent flames. It is the future work to extend VM method to turbulent flames.

REFERENCES

[1] A. H. Lefebvre, 1985. “Fuel Effects on Gas Turbine Combustion – Ignition, Stability, and Combustion Efficiency”. *ASME Journal of Engineering for Gas Turbines and Power,* **107**, pp. 24-37.

[2] John P. Longwell, Edward E. Frost, and Malcolm A. Weiss, 1953. “Flame Stability in Bluff Body Recirculation Zones”. *Ind. Eng. Chem.*, **45**(8), pp. 1629-1633.

[3] E. E. Zukowski and F. E. Marbel, 1955. “The Role of Wake Transition in the Process of Flame Stabilization on Bluff Bodies”. *AGARD Combustion Researches and Reviews*, pp. 167-180.

[4] Guenther von Elbe and Bernard Lewis, 1949. “Theory of Ignition, Quenching and Stabilization of Flames of Nonturbulent Gas Mixtures”. *Third Symposium on Combustion Flame and Explosion Phenomena*, pp. 68-79.

[5] Bernard Lewis and Guenther von Elbe. *Combustion, Flames and Explosions of Gases*, Academic Press Inc., New York and London, pp. 220-224.

[6] Kurt Wohl, 1953. “Quenching, Flash-Back, Blow-Off: Theory and Experiment”. *Fourth Symposium on Combustion Flame and Explosion Phenomena*, pp. 68-89.

[7] Kenneth K. Kuo, 2005. *Principles of Combustion, Second Edition*, John Wiley & Sons, Inc., Canada, pp. 323-326.

[8] Chung K. Law, 2006. *Combustion Physics*, Cambridge University Press, New York, pp. 358-361.

[9] Irvin Glassman and Richard A. Yetter, 2008. *Combustion (Fourth Edition)*, Elsevier Inc., Burlington, San Diego and London, pp. 201-207.

[10] Bernard Lewis and Guenther von Elbe. *Combustion, Flames and Explosions of Gases*, Academic Press Inc., New York and London, pp. 223.

[11] Beth Anne V. Bennett, Joseph Fielding, Richard J. Mauro, et al., 1999. “A comparison of the structures of lean and rich axisymmetric laminar Bunsen flames: application of local rectangular refinement solution-adaptive gridding”. *Combust. Theory Modelling* **3**, pp. 657–687.

[12]Irvin Glassman and Richard A. Yetter, 2008. *Combustion (Fourth Edition)*, Elsevier Inc., Burlington, San Diego and London, pp. 161-168.

[13] Yang Shiming and Tao Wenquan, 2005. *Heat Transfer, Second Edition*, Higher Education Press, Beijing, pp. 143-146 (in Chinese).

[14] Kenneth K. Kuo, 2005. *Principles of Combustion, Second Edition*, John Wiley & Sons, Inc., Canada, pp. 326-329.

[15] J. Buckmaster, P. Clavin, A. Linan, et al., 2005. “Combustion theory and modeling”. *Proceedings of the Combustion Institute* **30**, pp. 1–19.

[16] Irvin Glassman and Richard A. Yetter, 2008. *Combustion (Fourth Edition)*, Elsevier Inc., Burlington, San Diego and London, pp. 714.